

SCIENCE AND TECHNOLOGY OF WEAR-PROTECTIVE COATINGS FOR COMPUTER DISK DRIVE, CUTTING TOOL AND OTHER TRIBOLOGICAL APPLICATIONS*

Yip-Wah Chung

Department of Materials Science and Engineering
Northwestern University, Evanston, Illinois 60208, USA

ABSTRACT

Wear-protective coatings are used in computer disk drives, cutting tools and other tribological applications. Each application has different property objectives for the protective coating. Therefore, one must tailor-design such coatings for individual applications.

This paper presents two examples to illustrate the science and technology involved in the development of these wear-protective coatings. The first example is the development of TiN/SiN_x multilayer coatings for high temperature and rolling contact fatigue applications.

Using dual-cathode reactive sputtering, we were able to obtain TiN/SiN_x multilayer coatings with an equiaxed grain structure (rather than the usual columnar structure), which is crucial in improving rolling contact fatigue lives. More important, by optimizing the individual layer thickness in this system, we provide strong evidence that the multilayer structure is preserved up to 1000°C. This suggests that these coatings may be useful for high-temperature applications. The second example is the development of ultrathin protective overcoats for hard disks with extremely high storage density. The objective is to develop 2 nm thick overcoats, which must provide both wear and corrosion protection. In this case, this requires the coating to be atomically smooth and pinhole-free and at the same time to be compatible with the lubricant used in this application.

It is shown that nitrogenated carbon (CN_x), when deposited under optimal pulsed dc conditions, can satisfy all these requirements down to 1- 2 nm.

1. INTRODUCTION

Wear-protective coatings are used in various tribological applications such as gears, bearings, seals, cutting tools and computer disk drives. Depending on each specific application, the requirements are different.

By definition, one requires the coating to be adherent, tough and wear-resistant. In many applications, one prefers the coating to be smooth, to be deposited at relatively low temperatures and to be compatible with materials in contact. Many coating-deposition techniques are available that satisfy the above requirements, including chemical vapor deposition, thermal/plasma spraying, sputtering and cathodic arc methods.

Each technique has its own strengths and weaknesses. Coatings reported in this paper were deposited by magnetron sputtering.

2. MAGNETRON SPUTTERING

In magnetron sputtering, one places a target in a vacuum chamber, which is backfilled with a process gas such as argon. A negative high voltage is then applied to the target, which is mounted in front of a system of magnets. This results in the generation of an intense plasma. Positive ions in the plasma accelerate towards the target, sputter atoms from the target and deposit them onto the substrate. In reactive sputtering, the process gas contains a reactive component that reacts with target atoms to form the material of interest. In this technique, one has control over a large number of process parameters, viz. target power, total pressure, partial pressure of the reactive component, substrate temperature and bias. In some cases, one can synthesize multilayer coatings by having additional targets. When properly synthesized, multilayer coatings have been known to have properties that are better than expected from the rule of mixtures. This wide range of control gives magnetron sputtering an enormous advantage in coating synthesis and therefore in synthesizing coatings for a wide range of applications.

In this paper, we will present two examples to demonstrate how one optimizes deposition conditions to produce protective coatings with enhanced properties. The first example deals with the synthesis of TiN/SiN_x multilayer coatings for bearing and high-temperature tribological applications. The second example is the synthesis of CN_x coatings for use as protective overcoats in computer disk drives.

3. TiN/SiN_x MULTILAYER COATINGS WITH IMPROVED FATIGUE LIFE AND THERMAL STABILITY

3.1 Why TiN/SiN_x Multilayers?

Titanium nitride (TiN) has been widely used in protective coatings for bearings, gears, and cutting tools due to its good wear resistance, excellent thermal expansion match and inertness to steels. However, TiN coatings predominantly grow with a columnar grain structure. These columnar grain boundaries become the sites for crack initiation, resulting in premature failure of TiN coatings [1,2]. Therefore, the columnar structure of TiN coatings should be eliminated. Maintaining a fine equiaxed microstructure throughout the coating thickness is hence highly desirable and should significantly enhance its tribological performance. To accomplish this, we periodically interrupt TiN growth with nanolayers of a different material (SiN_x) to force TiN to renucleate [3], thus producing TiN/SiN_x multilayer coatings. In addition to suppressing columnar growth, these multi-

* This work is supported by the National Science Foundation and the National Storage Industry Consortium.

layer coatings offer an additional advantage over traditional coatings. There is ample evidence from the literature demonstrating that with proper choice of components, the hardness of a multilayer coating can be enhanced over the average of the two components [4-8].

We chose SiN_x for two reasons. First, SiN_x has an amorphous structure stable up to 1100°C [9]. Because of this amorphous structure, TiN is forced to renucleate each time a thin SiN_x layer is deposited. Second, Veprek et al. [10] showed that a nanocomposite coating made of a mixture of nanocrystalline TiN and amorphous Si_3N_4 attains hardness ≥ 50 GPa and is resistant against oxidation in air up to 800°C . Veprek et al. [10] attributed this high hardness to the small crystalline size (which suppresses dislocation motion and multiplication) and amorphous Si_3N_4 boundaries (which pin dislocations). Their studies showed that the Si content and TiN crystalline size must be controlled precisely to obtain the high hardness. Our multilayer approach is a better technique to grow TiN/ SiN_x coatings with better control of the crystallite size.

3.2 EXPERIMENTAL DETAILS

TiN/ SiN_x multilayer coatings were deposited in a dual-cathode unbalanced reactive magnetron sputtering system using standard 2-inch titanium and silicon targets (both 99.95% purity). An argon-25 % nitrogen mixture at a total pressure of 3 mTorr was used. Si (100) wafers and M2 steels were used as substrates. A TiN buffer layer of 80 nm was laid down without substrate bias prior to TiN/ SiN_x coating deposition. No deliberate substrate heating was applied. The coating thickness was set at $0.35 \mu\text{m}$. To minimize charging, we applied pulsed bias voltages to the Si target (2 kHz) and the substrate (20 kHz) during deposition. The duty cycle was typically 80%, with the positive bias set at 10% the absolute value of the negative bias.

The coating thickness and substrate curvature were measured using the Tencor profilometer, from which one calculates the internal stress via the Stoney equation [11]. All stresses measured were compressive. The structure was investigated by x-ray diffraction (XRD) using the $\text{Cu K}\alpha$ radiation at 0.154 nm. The root-mean-square (RMS) roughness was obtained by atomic force microscopy (AFM) over sampling areas of $1 \mu\text{m} \times 1 \mu\text{m}$ to $10 \mu\text{m} \times 10 \mu\text{m}$. The Hysitron nanoindenter was used to measure the hardness of these coatings as a function of indentation depth. This is to ensure that the hardness data we presented are not influenced by the substrate. Generally, this means that the indentation depth should not exceed 10 – 15 % of the coating thickness.

3.3 RESULTS AND DISCUSSION

Fig. 1 shows a cross-sectional TEM picture of a TiN/ SiN_x multilayer coating deposited at a substrate bias of -90V , with 2.0 nm TiN and 0.5 nm SiN_x layer thickness. Note the columnar structure of the TiN buffer layer and its disappearance within the TiN/ SiN_x multilayer coating. This clearly demonstrates the effectiveness of our approach in suppressing columnar growth.

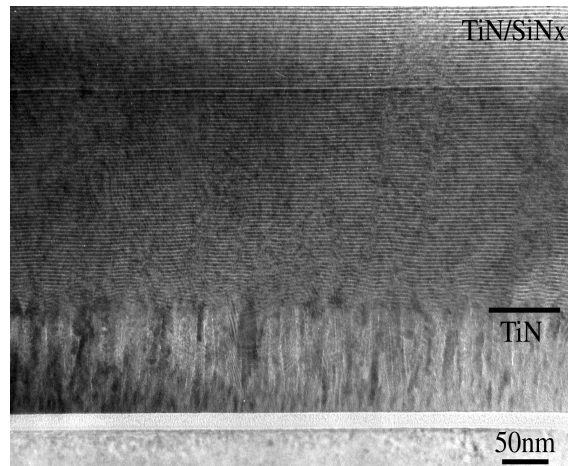


Fig. 1. Cross-sectional TEM micrograph of TiN/ SiN_x coating with TiN = 2.0 nm, SiN_x = 0.5 nm, substrate bias = -90V . The buffer layer is TiN.

Fig. 2 shows the variation of hardness versus the SiN_x layer thickness (TiN layer kept constant at 2.0 nm). The hardness of pure TiN is about 25 GPa and that of pure SiN_x is about 16 GPa. The multilayer coatings have hardness well above the average. At an SiN_x layer thickness of 0.5 nm, one attains a maximum hardness of about 45 GPa, about twice the value based on the rule of mixtures. The hardness improvement of multilayer coatings over their pure components has been observed in many systems.

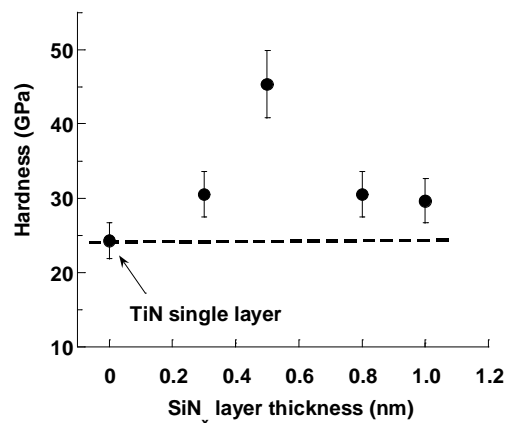


Fig. 2. Hardness of TiN/ SiN_x multilayer coatings versus SiN_x layer thickness, with TiN layer thickness = 2.0 nm and substrate bias = -90V .

We have further shown that these multilayer coatings are smoother, have lower coefficient of friction (under dry sliding against steels) and lower internal stress than their individual components. Under similar sliding conditions, TiN/ SiN_x multilayer coatings have wear rates about three to four times lower than the best TiN coatings. We have also applied these same coatings to bearings and subjected them under high-speed high-stress contact fatigue testing. These multilayer coatings achieve fatigue life at least eight times better than TiN under identical testing conditions (Fig. 3).

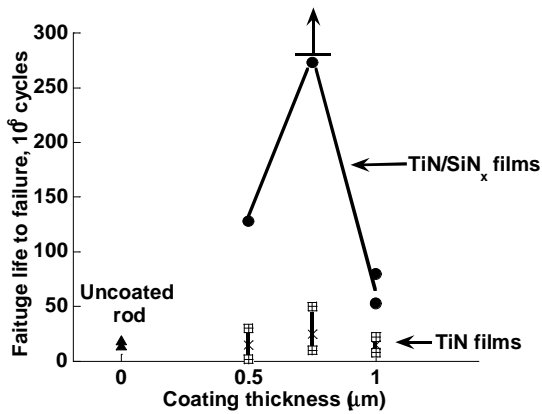


Fig. 3. Fatigue life of rolling contact fatigue test rods coated with TiN/SiN_x coatings and uncoated rods as a function of coating thickness. TiN layer thickness = 2.5 nm, SiN_x layer thickness = 0.5 nm. The arrow for the 0.75 micron thick TiN/SiN_x coating implies that the coating has not failed. Fatigue life data for rods coated with pure TiN coatings obtained by Polonsky et al. [2] using the same machine are also plotted for comparison.

The improved wear and fatigue life performance of TiN/SiN_x over pure TiN can be attributed to at least four reasons. First, because of the nanoscale crystallite size, it is difficult to nucleate dislocations in these coatings. Second, on the atomic scale, interfaces acts as obstacles to dislocation motion across layers. On the micron scale, interfaces cause crack deflection. Third, because of their lower intrinsic stress, the multilayer coatings are more resistant against adhesive failure (delamination). Finally, because of their equiaxed microstructure, the flaw size of TiN/ SiN_x multilayer coatings is generally in the nanometer range, compared with ~ 10-50 nm for columnar TiN coatings. Therefore, the stress intensity factor (proportional to the square root of the flaw size) is substantially smaller in multilayer coatings.

4. APPLICATION OF CN_x AS PROTECTIVE OVERCOATS IN COMPUTER DISK DRIVES

4.1 Protective Overcoats

The computer hard-drive industry is currently developing the necessary technologies to achieve an areal storage density of 100 Gbits/inch². In order to achieve such a density, a total magnetic spacing (distance between the pole piece of the read-write head and the top of the magnetic media layer) of only 10 nm is allowed. Within this spacing budget, the hard-disk overcoat thickness must be 2.0 nm or less. At this thickness, having an atomically smooth coating with low defect density is as crucial as the tribological performance of the coating.

A well-established method to reduce the defect density in films is low-energy ion bombardment during deposition [12]. One possible candidate material for these ultrathin overcoats is nitrogenated carbon, hereafter referred as CN_x. These CN_x films have many desirable properties. They have excellent tribological performance [13-16], can be grown with subnanometer surface roughness and are compatible

with existing lubricants and manufacturing technologies. In this paper, we report on the synthesis and corrosion performance of ultrathin CN_x films grown by magnetron sputtering.

4.2 Experimental Details

CN_x films were grown using dc magnetron sputtering in a single cathode deposition chamber at room temperature. The base pressure of the chamber was < 1×10⁻⁵ Pa.

Graphite (purity 99.995%) was used as the target material (5-cm diameter disk), and an Ar-5% N₂ mixture was chosen as the process gas. During deposition, the total pressure was kept at 0.5 Pa, and the target power was fixed at 200 watts. The films were grown on polished silicon (001) and 80 nm-permalloy-coated silicon substrates, the latter for corrosion tests. Prior to deposition, substrates were cleaned in situ by reverse-sputter etching in an argon plasma at 8 Pa with -500V bias.

The total CN_x film thickness was varied between 0.5 nm and 30 nm. In order to enhance ion bombardment of the growing film, a negative bias was applied to the substrate during growth. This bias was varied between 50 and 300V. During the initial runs, the substrate polarity was switched between the set negative bias and +50V using a low-frequency (200Hz) pulse generator.

For subsequent runs, high-frequency pulse generators were connected to both the target and the substrate power supplies. These pulse generators switch the polarity of the target and the substrate at a fixed frequency of 20 and 2 kHz respectively. In this case, the voltage applied in the positive cycle is set at 10 % of that applied in the negative cycle.

Corrosion tests were carried out to evaluate the defect density of these ultrathin films. In this test, films grown on permalloy-coated silicon substrates were dipped into a buffered 0.5 M NaCl solution for 24 hrs at room temperature. The samples were then taken out of the solution, rinsed in deionized water and dried with dry nitrogen.

They were then examined under an optical microscope at 100 times magnification for corrosion damage, which is usually in the form of spots. The number of spots in a 0.77 mm² (equivalent to 3" × 4" after 100× magnification) area was counted and used as a measure of the corrosion performance of the overcoat.

4.3 Results and Discussion

Fig. 4 shows the effect of film thickness on the corrosion spot density in the films. In this plot, the shaded region represents the maximum acceptable corrosion damage for protective overcoats used in today's hard drives.

Without substrate bias, the corrosion performance of CN_x films was not acceptable below a thickness of 10 nm (data not shown). Application of a low-frequency bias to the substrate improves the corrosion resistance; however, the corrosion performance at thickness less than 4 nm is still unacceptable.

With higher frequency bias applied to both the target and the substrate, the corrosion performance of CN_x films is acceptable down to a thickness ~1.0 nm.

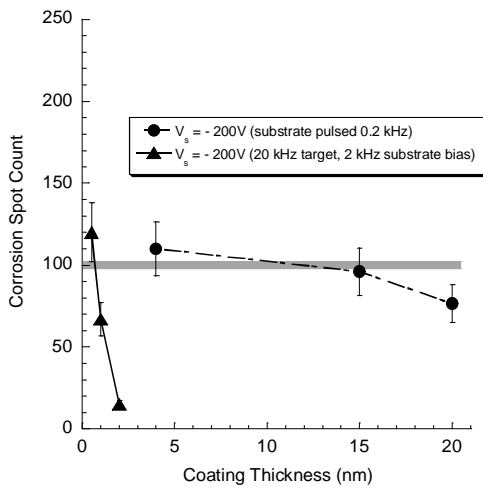


Fig. 4. Variation of the corrosion spot density with CN_x film thickness. (●) Low-frequency (200Hz) pulse bias on the substrate only and (▲) 20kHz pulse bias on target and 2 kHz pulse bias on substrate. The shaded region represents the maximum acceptable corrosion damage of an overcoat used in today's hard-drives.

Fig. 5 shows two micrographs, one from a ~1.0 nm CN_x coated permalloy/Si substrate and the other from an uncoated permalloy/Si substrate after corrosion testing. It can be seen that severe corrosion damage has occurred on the surface of the bare permalloy/Si substrate.

These results indicate that low-energy ion bombardment of the growing film has a significant effect on film properties. Bombardment of the substrate surface by low-energy ions increases the mobility of surface species, which in turn improves surface roughness, increases film density and reduces the number of pinhole defects [17-19]. Obviously, one would not realize these beneficial effects if the ion bombardment energy were too low or too high. We have experimented with a range of energies. It appears that ion bombardment at 100-200 eV in our deposition system produces the best results.

Additionally, process parameters were adjusted such that the mean free path of impinging ions (primarily Ar⁺) was greater than the anode dark space width. The dark space is the region above the substrate surface where there is little or no ionization. This is the region where the impinging ions "see" the negative potential on the substrate and accelerate toward it. In our studies, the pressure and other operating conditions were chosen such that the dark space width was ~ 2 mm, whereas the mean free path of the ions was ~ 15 mm (>> dark space width). This resulted in approximate monoenergetic ion bombardment of the growing film.

Depending on the nitrogen content, CN_x films can have relatively high electrical resistivity [14]. During reactive sputtering, CN_x forms not only on the substrate, but also on some parts of the graphite target. It is therefore possible that local charging may occur on the substrate and the target. Such local charging can result in variable ion bombardment energy and arcing. The former results in less than optimum

film properties, while the latter may produce macroparticles. The pulsed dc bias to the substrate and the target minimizes these problems. The negative cycle functions in the usual way (ion bombardment), while the positive cycle draws low-energy electrons from the plasma to neutralize the surface charge. Note that a side benefit of pulsed dc power is enhanced plasma ionization at some optimum pulse frequency (~10 kHz). This enhancement is primarily a result of the different time constants in the generation and loss of ions in the magnetron plasma [20,21]. Under these optimal conditions, the RMS roughness of 50 nm thick CN_x films grown on polished silicon substrates (RMS roughness = 0.07 nm) was measured to be less than ~0.09 nm using atomic force microscopy (1.0μ × 1.0μ).

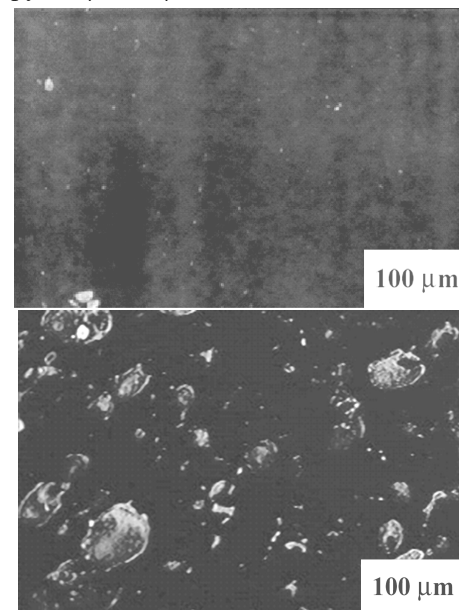


Fig. 5. Optical micrographs of uncoated permalloy/Si substrate (left) 1 nm CN_x coated permalloy/Si sample taken after corrosion testing. The spots are due to corrosion damage. Image contrast has been inverted for clarity.

5. CONCLUSIONS

In this paper, we demonstrate the use of SiN_x to interrupt TiN growth to produce equiaxed TiN/SiN_x multilayer coatings. These coatings are twice as hard as pure TiN coatings, are significantly smoother and have lower internal compressive stresses than columnar TiN coatings. Under optimum conditions, these TiN/SiN_x multilayer coatings have tribological properties (sliding and rolling) much improved over TiN.

To obtain functional overcoats for extremely high-density recording, one needs to obtain smooth and pinhole-free ultrathin overcoats. We show that these properties can be satisfied by CN_x films deposited using magnetron sputtering of graphite in argon/nitrogen, provided that (i) appropriate pulsed dc voltages are applied to the target and the substrate, and (ii) the dark space width is much less than the mean free path of impinging ions. Acceptable corrosion performance can be obtained by CN_x down to a thickness of 1 nm.

REFERENCES

1. I. A. Polonsky, T. P. Chang, L. M. Keer, and W. D. Sproul, *Wear*, 208 (1997) 204.
2. I. A. Polonsky, T. P. Chang, L. M. Keer, and W. D. Sproul, *Wear*, 215 (1998) 191.
3. M. M. Lacerda, Y. H. Chen, B. Zhou, M. U. Guruz, and Y. W. Chung, *J. Vac. Sci. Technol. A*, 17 (1999) 2915.
4. S. A. Barnett and M. Shinn, *Ann. Rev. Mater. Sci.*, 24 (1994) 481.
5. X. Chu and S. A. Barnett, *J. Appl. Phys.*, 77 (1995) 4403.
6. A. Madan, Y. Y. Wang, S. A. Barnett, C. Engstrom, H. Ljungcrantz, L. Hultman, and M. Grimsditch, *J. Appl. Phys.*, 84 (1998) 776.
7. S. L. Lehoczky, *J. Appl. Phys.*, 49 (1978) 5479.
8. J. S. Koehler, *Phys. Rev. B*, 2 (1970) 547.
9. S. Veprek, *J. Vac. Sci. Technol. A*, 17 (1999) 2401.
10. S. Veprek, S. Reiprich, and S. H. Li, *Appl. Phys. Lett.*, 66 (1995) 2640.
11. M. Ohring, *The Materials Science of Thin Films*, Academic Press, New York, 1992, p. 416.
12. S. M. Rossnagel and J. J. Cuomo, *Thin Solid Films* 171, (1989) 143.
13. W. C. Chan, B. Z. Zhou, Y. W. Chung, C. S. Lee, and S. T. Lee, *J. Vac. Sci. Technol. A* 16 (1998) 1907.
14. M. Y. Chen, X. Lin, V. P. Dravid, Y. W. Chung, M. S. Wong, and W. D. Sproul, *Tribol. Trans.* 36 (1993) 491.
15. E. C. Cutiongco, D. Li, Y. W. Chung, and C. S. Bhatia, *J. Tribol.* 118 (1996) 543.
16. A. Khurshudov, K. Kato, and S. Daisuke, *J. Vac. Sci. Technol. A* 14 (1996) 2935.
17. W. Ensinger, *Nucl. Instrum Methods* 127 (1997) 796.
18. L. Hultman, W. D. Munz, J. Musil, S. Kadlec, I. Petrov, and J. E. Greene, *J. Vac. Sci. Technol. A* 9 (1991) 434.
19. A. S. Kao and G. L. Gorman, *J. Appl. Phys.* 67 (1990) 3826.
20. S. Ashida, C. Lee, and M. A. Lieberman, *J. Vac. Sci. Technol. A* 13 (1995) 2498.
21. S. Ashida, M. R. Shim, and M. A. Lieberman, *J. Vac. Sci. Technol. A* 14 (1996) 391.